Physicochem. Probl. Miner. Process., 58(6),2022, 154951

http://www.journalssystem.com/ppmp

Physicochemical Problems of Mineral Processing

ISSN 1643-1049

Dispersion of sodium phytate on muscovite and the implications for arsenopyrite flotation

Dan Zou [1], Zhen Wang [1], Kaile Zhao [2], Ying Xu [1]

[1] School of Environment and Resource, Southwest University of Science and Technology, Mianyang 621010, China

[2] Institute of Multipurpose Utilization of Mineral Resources, Chinese Academy of Geological Sciences, Chengdu

Corresponding author: wangzhen@swust.edu.cn (Zhen Wang), zhaokaile0557@sina.com (Kaile Zhao)

Abstract: The effective flotation separation of sulfides and sliming silicate minerals is always a difficult problem. In this paper, the selective flotation of arsenopyrite from muscovite was studied by using sodium phytate (SP) as dispersant, and the mechanism was investigated through SEM/EDS, zeta potential, FTIR and XPS measurements. Single mineral flotation results showed that with the increasing isoamyl xanthate (IAX) dosage the recovery of arsenopyrite increased, until 8×10-5 mol/L IAX (79.40% recovery, pH=7), after that it decreased slightly. While muscovite floated poorly at any IAX concentration. For the mixed minerals, arsenopyrite recovery was only 54.63% while that of muscovite was 42.70%, which was attributed to the coverage of muscovite on arsenopyrite surface. When 6×10^{-5} mol/L SP was added into the mixed minerals system, the recovery of arsenopyrite recovered to 68.26% while that of muscovite was 8.48% (approximate the value of the single mineral). SEM/EDS results showed that SP could disperse muscovite and prevented its coverage on arsenopyrite surface. Zeta potential results showed that the electrokinetic potential of muscovite and arsenopyrite decrease from -26.60mV to -39.01 mV and from -26.90 mV to -27.84 mV at pH=7, respectively. It was obvious that the negatively charged phytate ions selectively adsorbed on the surface of muscovite. FTIR and XPS resulted co-proved the chemisorption of SP with active sites on muscovite while arsenopyrite spectrum did not change significantly, which was consistent with flotation and zeta potential results. The selective adsorption of SP on muscovite compared to arsenopyrite was responsible for the effective separation of them.

Keywords: cassiterite, chlorite, sodium oleate, carboxymethyl cellulose, selective inhibition

1. Introduction

Dulan Jinhui Mining Co. LTD consists of two concentrators, which locates in the Qinghai Province, Western China and have a processing capacity of 4000 t/d. It is the largest gold producer in Qinghai Province. The gold-bearing mineral in the dressing plant is mainly arsenopyrite, but the associated clay mineral content is up to 37%, and is mainly muscovite ($KAl_2(AlSi_3O_{10})(OH)_2$), layered silicate mineral) (Wang et al., 2021; Zhao et al., 2020).

The gold content of the ore need to be enriched to made it easier to extract gold later in the smelting process. From the angle of environmental protection, bioleaching was applied in some concentrators (Zhang et al., 2021; Thakur et al., 1995). However, the long experiment period and the strict requirements of microorganisms on the living environment limited the microorganism induced beneficiation (Lopéz et al., 2019). In the beneficiation experiment, the researchers found that the surface properties of sulfide ore and clay were very different. Taking advantage of that flotation had become the most widely used beneficiation method for gold sulfide ore.

In sulfide type metal ore, muscovite, chlorite and serpentine are the common clay minerals associated with the valuable minerals, which can easily mixed into the sulfides concentrate during the flotation (Feng et al., 2012). The main reason for the entrainment was that clay minerals such as muscovite tend to produce slime in the process of grinding. These clay mineral slimes in slurry was easy to adsorb on the surface of sulfide minerals, resulting in a significant reduction in the recovery of sulfide minerals (Chen and Peng, 2018).

DOI: 10.37190/ppmp/154951

About the methods used to remove clay minerals from sulfide mineral surface, high strength agitation (Chen et al., 2017) and introducing high power pulse in the process of flotation are the two that must be mentioned, but they all had high energy consumption (Chanturiya et al., 2011). Some people try to use complexing collectors in sulfide ore flotation to solve this problem, but the effect was poor (Ferlin et al., 2015). At the same time collector MTKH (perhydro-1,3,5-ditiazin-5-yl-methane) and activator Fe^{3+} were also developed and introduced into the flotation experiment (Chanturia et al., 2015; Deng et al., 2021). Clay minerals will adsorb to the surface of sulfide ore, thus reducing the adsorption of sulfide ore and collector. So dispersants have also been used to eliminate the effects of clay minerals during sulfide ore flotation. The sodium hexametaphosphate (SHMP) is one of the most widely used industrial dispersants in flotation of copper-nickel ores containing serpentine (Feng et al., 2018). Oxalic acid is also used to disperse the adsorption of clay minerals and sulfide minerals (Tang et al., 2020). It was found that after conditioning with oxalic acid, serpentine became negatively charged, the same as sulfide minerals, inducing repulsion forces between sulfide minerals and serpentine. However, to obtain a satisfactory selection index, the copper-nickel sulfide ore (containing multiple serpentine) required a very high dispersant and collector dosage (Ramirez et al., 2018). In recent years, it was proposed to introduce organic dispersants such as xanthan gum, lemon yellow and galactomannan into the flotation process. These organic dispersants could decrease the zeta potential values of serpentine to some extent, but the influence was low even at high dosages (Ming et al., 2020; Zhang en al., 2020).

In the present study, a sodium salt of phytic acid named sodium phytate (SP, $C_6H_6Na_{12}O_{24}P_6$), was employed as the muscovite dispersant in the flotation of muscovite/arsenopyrite mineral system for the first time. SP is a natural antioxidant, color-protecting and environmentally friendly food additive with extensive source (existing beans and cereals) (Zhang et al., 2021). It exhibits a high affinity for some polyvalent cations. There are numerous phosphate groups (the functional group is P-O) in the molecule, which can easily ionize in the aqueous solution (Huang et al., 2018). SEM/EDS, Zeta potential, Fourier transform infrared spectrum (FTIR) and XPS measurements were used to reveal the dispersion mechanism of SP on fine muscovite adsorbed on the surface of arsenopyrite, also providing reference for the flotation separation of sulfide minerals from clay minerals.

2. Experimental

2.1. Samples and reagents

The arsenopyrite and muscovite used in the experiment were obtained from Dulan Jinhui Mining Co., LTD. A portion of the mineral samples were hand-picked and crushed before being ground in a porcelain ball mill. Then the grinding minerals were dry screened to obtain –74+45 μm components of arsenopyrite and –38 μm components of muscovite, respectively, for flotation test, particle size distribution analysis and XPS detection. Lastly, some of the fine particles were further ground to ~5μm and used for zeta potential and FTIR detection. The results of element analysis and X-ray diffraction spectra (XRD, Fig. 1) of samples indicated that the purity of the samples of arsenopyrite and muscovite were all > 96%, and met the requirement. The results of particle size distribution analysis (Fig. 2) indicated that > 50% muscovite particles was –19 μm, and ~20% lower than –10 μm, showing that it was appropriate to simulate the sliming clay minerals. Artificial mixed minerals were prepared by mixing arsenopyrite and muscovite samples at a mass ratio of 1:1.

The SP used in experiments were obtained from Rin En Technology Development Co., LTD. SP was a white powder with a molecular weight of 923.82, and was easy to dissolve in water. The molecular structures of SP is shown in Fig. 3. The pH regulators were sulfuric acid (H_2SO_4) and sodium hydroxide (NaOH). Terpineol (TP) was used as the frother. KCl was the back-ground electrolyte used in zeta potential measurements. Deionized water (18.2 MΩ·cm) was used for all tests.

2.2. Micro-flotation tests

XFGII type laboratory flotation machine with 60 ml cell was used in the micro-flotation experiments. A 2 g of single mineral samples and 38 ml deionized water were mixed in the flotation cell, and the rotation speed was adjusted to 1900 rpm. After stirring for 2 min, the pH regulator, desired dosage of dispersant, collector (8×10^{-5} mol/L) and frother (1×10^{-4} mol/L) were added into the pulp in sequence, with the

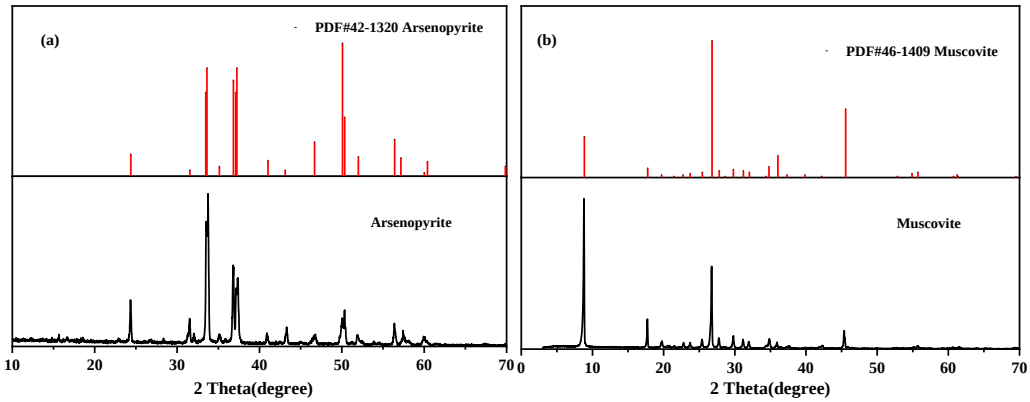

Fig. 1. X-ray diffraction patterns of (a) arsenopyrite and (b) muscovite

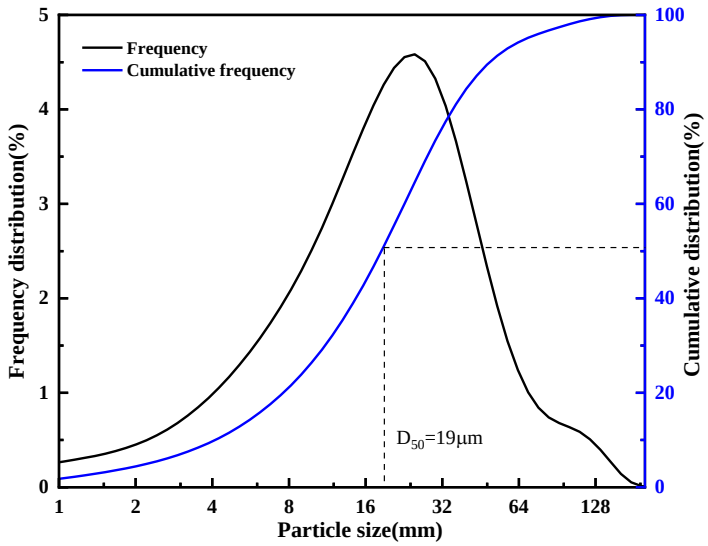

Fig. 2. Size distribution of the muscovite particles

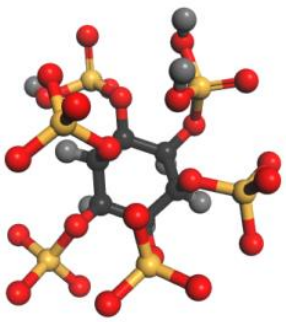

Fig. 3. Molecular structures of SP ($C_6H_6Na_{12}O_{24}P_6$)

interval of 3 min, respectively. After 4 min of flotation, the concentrate and tailings were collected, filtered and dried. For single mineral flotation, the flotation recovery was calculated based on mass balance. For flotation tests of mixed minerals, the flotation recovery was calculated based on solid weight ratio and As grade between two products. Three flotation tests were made under the same experimental conditions, and the average values were reported.

2.3. SEM/EDS analysis

The single arsenopyrite and muscovite samples were detected directly to qualitatively obtained particle shape, respectively. For mixed arsenopyrite/muscovite system, the flotation concentrates of mixed

minerals without and with 6×10^{-5} mol/L SP at pH 7 were collected and scanned to obtain the information of particle agglomeration and dispersion.

Morphology and local (Energy Disperse Spectroscopy) EDS spectra of the samples were obtained using (scanning electron microscope) SEM (Zeiss-Sigma 300, German) equipped with an EDS detector (X-MAX 20, UK). The main operating parameter were 10 kV EHT (acceleration voltage), 8.1 mm WD (working distance) and 5.0 KX Mag (magnification times).

2..4. Zeta potential measurements

A 30 mg of mineral powders was added to 50 mL KCl aqueous solution (1 mM) to obtain a suspension, and then conditioned it through magnetic agitation. During stirring, the desired pH regulator, dispersant and collector were added separately to the beaker in sequence, then conditioned for 10 min. After stopping the stirring, at least 30 min was allowed for precipitation. A Delsa 440sx Zeta Potential Analyzer (Malvern Instruments Ltd, United Kingdom) was used for the measurement of the zeta potential. The average of at least three independent experiments and the standard deviation of parallel results were calculated and presented.

2.5. FTIR measurements

KBr diffuse reflectance method and IRAffinity-1 Fourier transform infrared spectrometer (shimadzu, Japan) were used to obtain the spectra of mineral samples before and after treatment with flotation reagent(s). Ultrasound was performed on 30 mg pure mineral sample (~5μm) in 100 ml deionized water. Reagents were then added in the order as that in flotation tests (SP = 6×10^{-5} mol/L, IAX = 8×10^{-5} mol/L). The pulp was stirred at 25°C (pH 7) with a magnetic agitator for 30 min, then centrifuged at 4500 rpm. The precipitation was washed with deionized water for 3 times and dried in a vacuum oven. In the end, the dry mineral samples were collected for infrared detection at room temperature. The wave number of the spectrum ranges from 400-4000 cm^{-1}. Each spectrum recorded 20 scans at a resolution of $4cm^{-1}$.

2.6. XPS detections

A Thermo Scientific K-Alpha spectrometer (United States) was used for the determination of the XPS spectra of the arsenopyrite and muscovite powders. The pressure in the analysis chamber was less than 5×10−7 mbar. Al Kα X-rays with 1486.6 eV of energy and 12 kV×15 mA of power for narrow scans were employed for observations. The minerals before and after reagent treatment were dried in a vacuum oven and then tested at ambient temperature. The C1s peak refers to the binding energy (BE) of an uncharged hydrocarbon at 284.8 eV. The detection process was carried out in FAT mode, and the spectrometer was calibrated with Cu2p3/2/ (932.67 eV), Ag3d5/ (368.30 eV), and Au4f7/2/ (84.00 eV) standard samples. XPS Peak Fit software (version 4.1) was used for data fitting.

3. Results and discussion

3.1. Flotation tests

3.1.1 Single mineral flotation

Flotation tests of single minerals were performed to explore the effects of IAX dosage and pH upon the flotability of arsenopyrite and muscovite. The results are demonstrated in Fig. 4. In the preliminary exploration experiment, the optimal dosage of frother dosage was 1×10^{-4} mol/L, but considering the space problem, the curve of frother dosage and flotation recovery rate was not included in the manuscript. As illustrated in Fig. 4(a), arsenopyrite showed good flotability in the pH range of 4-10, while muscovite was unfloatable in the xanthate system, conforming to previous findings (Yu et al., 2019). When the concentration of IAX was higher than 8×10^{-5} mol/L, the recovery of arsenopyrite decreased slightly with the increasing concentration of collector, which might be due to the formation of double layer adsorption. Fig. 4(b) indicates that the flotability of arsenopyrite decreased sharply with the increase of pH. From the flotation of single mineral results, arsenopyrite and muscovite seems to be separated in xanthate system at pH < 10.

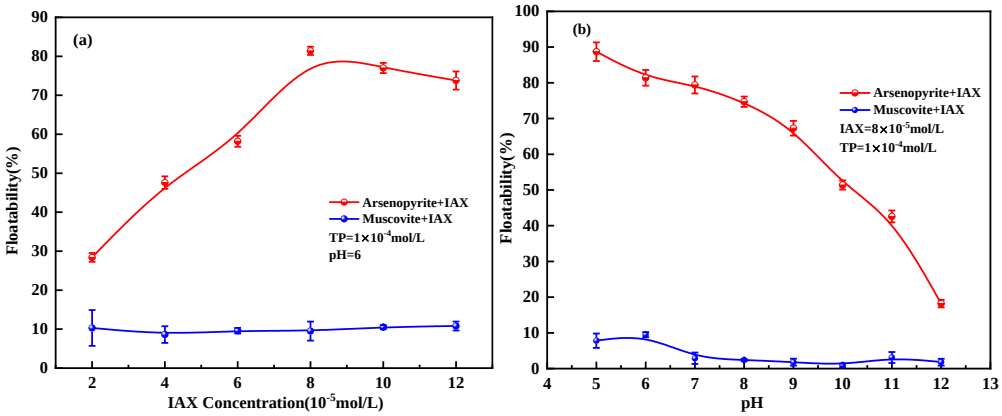

Fig. 4. Effects of (a) IAX concentration and (b) pH on recovery of arsenopyrite and muscovite

3.1.2. Flotation separation of artificial mixed minerals

The separation tests of artificial mixed minerals were conducted to investigate the effect of SP on the separation of arsenopyrite and muscovite mixtures (mass ratio of 1:1). Frother dosage was 1×10-4 mol/L. The results are listed in Fig. 5.

Fig. 5 demonstrates the effect of slurry pH and SP concentration on the separation of artificial mixed minerals. It can be seen that the recovery of arsenopyrite was only 54.63% and muscovite recovery increased to 42.70% without SP, suggesting the entrainment of muscovite with arsenopyrite and the adverse effect on its flotation (Wang et al., 2021). However, the flotation recovery of arsenopyrite increased to 68.26%（approximating the value of single flotation）and muscovite decreased to 8.48% with the addition of SP (6×10-5 mol/L) at pH 7. This indicated that SP can recover the flotability of arsenopyrite in artificial mixed flotation.

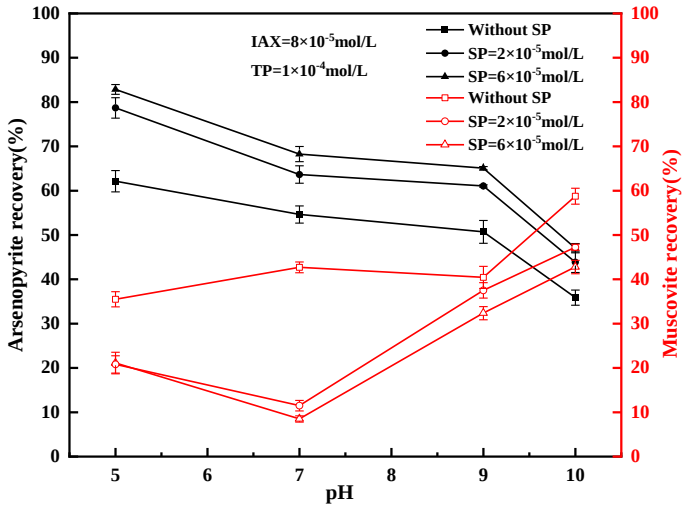

Fig. 5. Flotation recovery of mixed flotation separation

3.2. SEM and EDS results

SEM/EDS detections were employed to investigate the influence of the addition of 6×10-5 mol/L SP on the surface state of both minerals, thus on the flotability of them at pH 7.

As can be seen from Fig. 6(a) and (b), the morphology of arsenopyrite was semi-granular, while that of muscovite was flake (Deng et al., 2018). As is evident in Fig. 6(c), for the flotation concentrate of the mixed arsenopyrite/muscovite minerals without SP, the arsenopyrite particles were coated with numerous muscovite fines, and the muscovite fines and arsenopyrite fines were agglomerated. In the mixed flotation process, the slime coating or coagulation between muscovite and arsenopyrite which prevents the flotation of arsenopyrite particles, and results in the inclusion of muscovite into the concentrate (Wang et al., 2020). As shown in Fig. 6(d), for the flotation concentrate of the mixed

arsenopyrite/muscovite minerals with dispersant SP, the coagulation or slime coating between arsenopyrite and muscovite was reduced obviously. Therefore, SP could eliminate the heterocoagulation phenomenon in the slurry and improve the flotation of arsenopyrite, which verified the previous experimental results.

EDS spectrum of single arsenopyrite (Fig. 7(c)) show that the main elements were As, Fe and S. However, K, Al and Si (which correspond to the elemental composition of muscovite) can be easily found in EDS spectrum of artificial mixed mineral flotation concentrate. The content of As decreased obviously when SP was not involved (Fig. 7(b)). This indicated that muscovite floated with arsenopyrite and mixed into the concentrate. When SP was added in the flotation process, the content of As of the concentrate was restored to the level of single mineral (Fig. 7(a)), indicating that SP played a dispersive role.

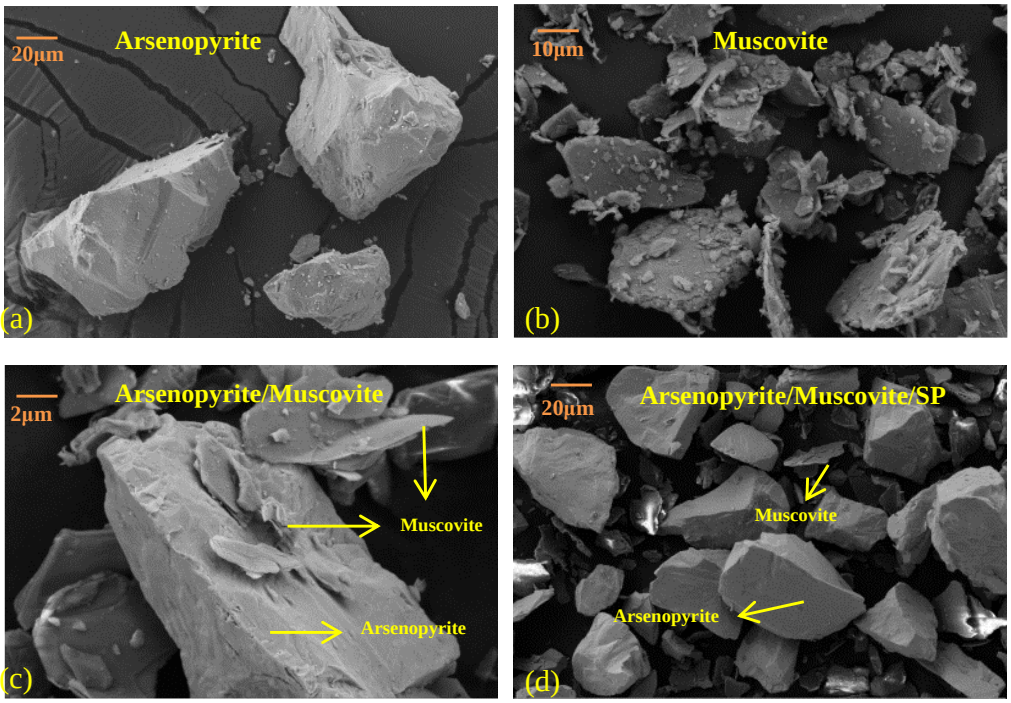

Fig. 6. The SEM images of (a) arsenopyrite and (b) muscovite, and (c) flotation concentrate without SP and (d) with SP

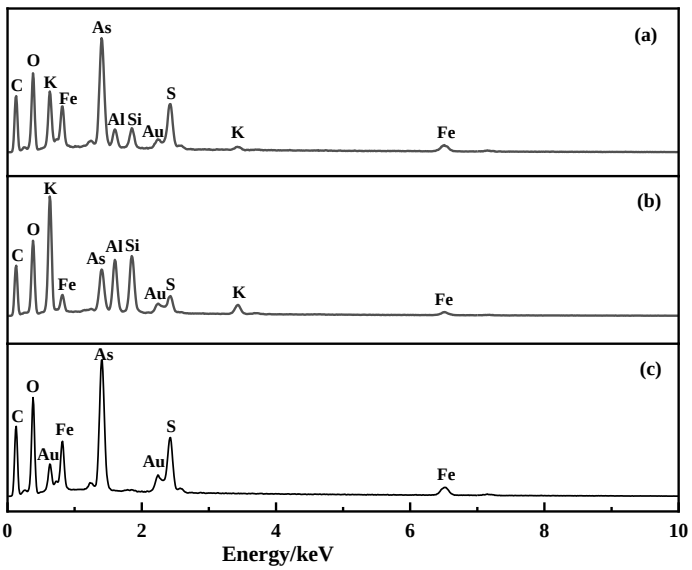

Fig. 7. EDS of (a) flotation concentrate with SP, (b) flotation concentrate without SP, (c) pure arsenopyrite

3.3. Electrokinetic potentials

The flotation results of artificial mixed minerals showed that SP affected the recovery of arsenopyrite and muscovite at pH 7 significantly. To investigate its mechanism, electrokinetic potential changes at the solid-liquid interface in the presence of different flotation reagents were investigated on the two minerals. The results are shown in Fig. 8.

Previous studies showed that the IEP (Isoelectric Point) of muscovite and arsenopyrite were near pH=1 and pH=2, respectively. The IEP of arsenopyrite and muscovite could not be detected in this study. For bare arsenopyrite and muscovite, the measured zeta potentials were consistent with previous measurements (Lu et al., 2019). Fig. 8(a) and (b) showed that after the interaction with xanthate, the zeta potentials of muscovite and arsenopyrite all decreased, but that of arsenopyrite droped more, indicating a stronger adsorption of xanthate on arsenopyrite compared to muscovite. This was consistent with the previous experimental results. After SP addition, the electrokinetic potentials of both minerals decreased (because of the adsorption of C6H6O24P612-), but the decrease of muscovite was more (~12.41 mV at pH 7), indicating that SP were well adsorbed on muscovite, while little adsorbed on arsenopyrite. The variation of Arsenopyrite+IAX and Arsenopyrite+SP+IAX was almost the same, showing that SP did not affect the subsequent adsorption of IAX on arsenopyrite surface.

It should be noted that previous studies had shown that heterocoagulation still occurred when two minerals had the same charge (Wang et al., 2013; Yao et al., 2016). In this study, arsenopyrite and muscovite were negatively charged at pH (2-12), but heterocoagulation may still occurred between them, as proved in Fig. 6.

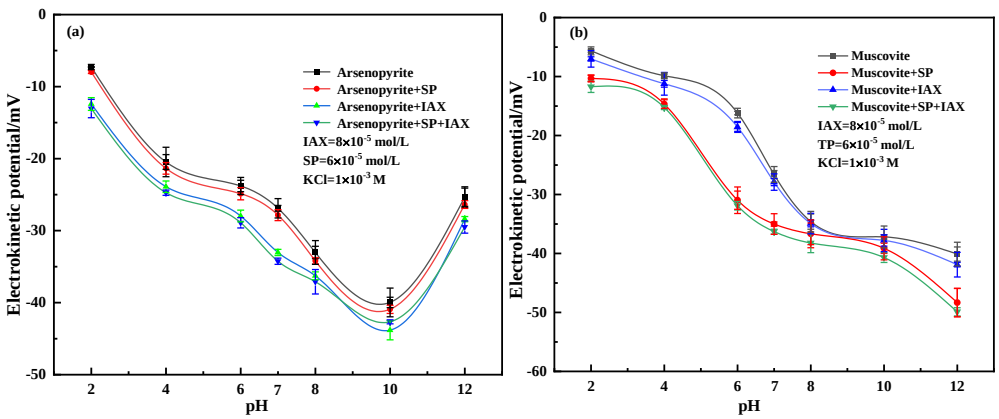

Fig. 8. Zeta potential values shown as a function of pH for (a) arsenopyrite and (b) muscovite

3.4. FTIR measurements

To better understand that how SP selectively absorbed on muscovite at pH 7.0, FTIR tests were conducted to detect the adsorption mechanism. The FTIR spectra of the two minerals before and after treatment with different reagent schemes were tested, and the results are shown in Fig. 9 to 11.

In Fig. 9, the absorption peaks at 870 and 1053 cm−1 in the spectra of SP can be attributed to the asymmetric and symmetric stretching of the P=O group, and that at 557 cm−1 corresponded to P-O-C stretching (Chen et al., 2018). This confirmed that P-O was the main functional groups in the SP molecule. For IAX, the peaks at 2922 and 2864 cm−1 corresponded to –CH2 and –CH3 stretching vibrations (Zhang et al., 2018; Huang et al., 2019).

The FTIR spectra of arsenopyrite and muscovite conditioned in different reagents at pH 7 are shown in Fig. 10 and Fig. 11. As shown in Fig. 10, at 3426 and 1636 cm−1 the bending vibrations of −O−H appeared. These were mainly from the adsorption layer containing water on arsenopyrite surface. At 1066 cm−1, the characteristic peak were the S-Fe antisymmetric stretching vibration. No distinct band shifts were observed in the spectra of arsenopyrite treated with SP, while the characteristic absorption peaks of the collector were evident. In the FTIR spectrum of IAX-treated arsenopyrite, the characteristic peak at 3426 cm−1 corresponding to –OH vibration shifted clearly to a higher frequency (3439 cm−1). According to this phenomenon, the –OH group was involved in adsorption, so hydrogen bond adsorption occurred. A peak shift of 27 cm−1 (from 1066 to 1039 cm−1) occurred, concluding that S-Fe

group was also involved. The stretching vibration characteristic peaks of –CH2/–CH3 were located at 2917 and 2843 cm−1. This indicated the physical and chemical adsorption of IAX on arsenopyrite surface. When conditioned with SP+IAX the characteristic peaks belonging to stretching vibrations of–CH2/–CH3 and S-Fe antisymmetric stretching vibration still presented at 2921 cm−1, 2852 cm−1 and 1039 cm−1, respectively, indicating that the adsorption of IAX on the arsenopyrite surface could not be hindered by SP pre-treatment.

However, for muscovite, it's totally different. As shown in Fig. 11(a), for muscovite treated with reagent or not, the bending vibrations of −O−H appeared at 3440 cm−1 (Wang et al., 2014). After treatment with IAX, apparently, the characteristic peak had no displacement, meaning no obvious adsorption taking place. After SP treatment, new characteristic peaks appeared at the wave numbers between 1000 and 500 cm−1. In order to more clearly discuss the adsorption of SP on the surface of muscovite minerals, the FTIR spectrum boundary was further narrowed. Fig. 11(b) shows that after SP treatment, the peaks located at 546, 529, and 515 cm−1 attributed to the asymmetric and symmetric stretching vibrations of P–O–C appeared. This suggests the chemisorption of SP on the muscovite surface. After SP+IAX treatment, the typical absorption bands of SP were still observed at 547, 531, and 514 cm−1, but the band at 2922 and 2864cm−1 (–CH2/–CH3 of IAX) were not discovered.

The results of the FTIR and zeta potential measurements reveal that SP was rarely adsorbed onto arsenopyrite surface, so it could not hinder the adsorption of IAX on arsenopyrite, but the SP molecules were largely adsorbed onto muscovite surface and resulting in the dispersion of fine muscovite that originally adsorbed on the surface of arsenopyrite. This dispersion of muscovite from arsenopyrite surface liberated the active sites for IAX adsorption, and the flotability recovered, as shown in Fig. 5.

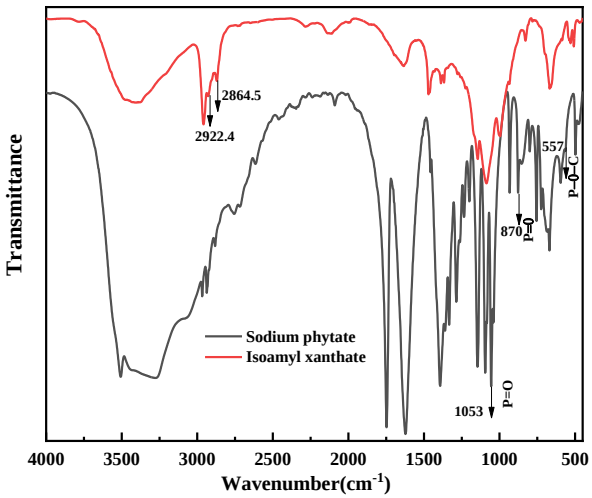

Fig. 9. FTIR spectra of SP and IAX used in this study

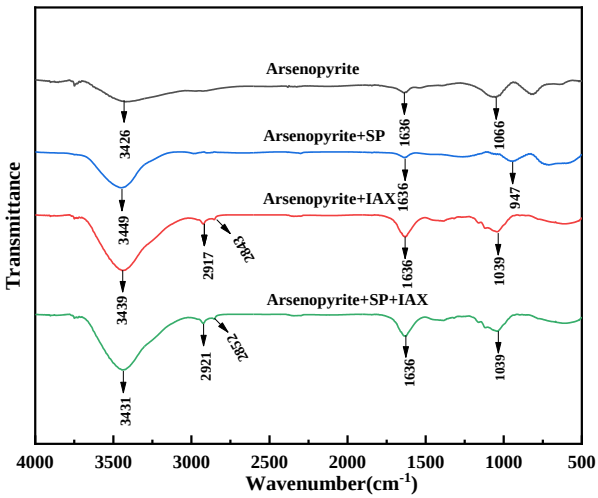

Fig. 10. FTIR spectra of arsenopyrite and arsenopyrite treated with SP, IAX, SP + IAX

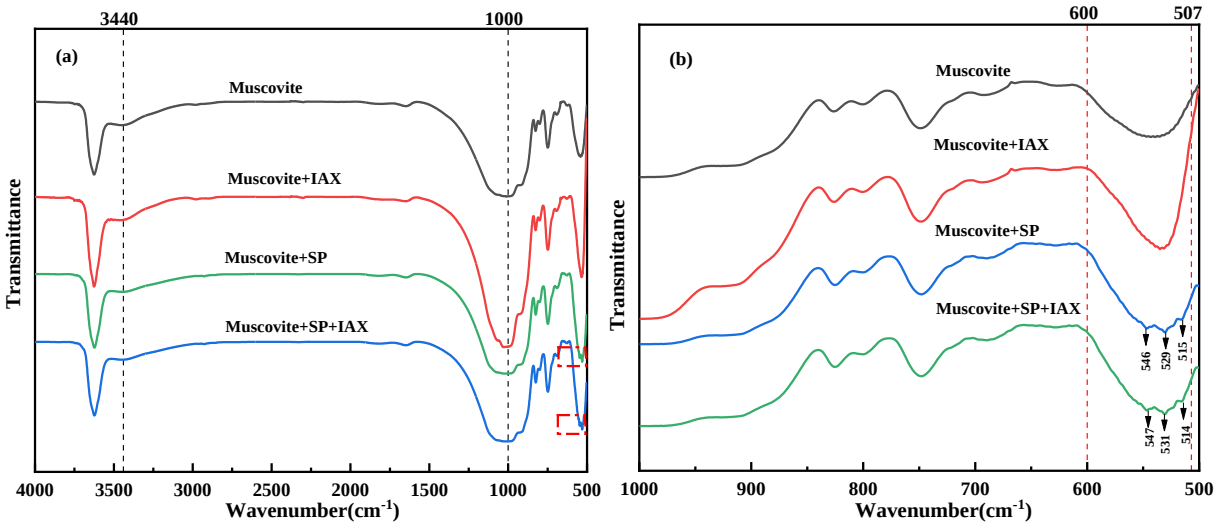

Fig. 11. FTIR spectra of (a) muscovite and muscovite treated with SP, IAX, SP + IAX, and (b) enlarged spectra range from 1000 to 500 cm^{-1}

3.5. XPS detection

After interaction with SP, the XPS full spectrum (a, b) of two minerals, and the XPS spectra of various elements on muscovite (c-e) and arsenopyrite surface (f-h) were drawn (Fig. 12). From the full spectrum of muscovite, the P characteristic peak was found on the muscovite surface after treatment with SP (Fig. 12(a)) while it did not occur on the arsenopyrite surface (Fig. 12(b)), which showed the considerable adsorption of P-containing SP on muscovite and almost no adsorption of SP on arsenopyrite.

XPS spectra of Al, Si and O of muscovite and Fe, As and O of arsenopyrite before and after treatment with SP are shown in Fig. 12c-h, and the corresponding binding energy and the binding energy shifts are listed in Table 1. The 0.41 eV shift of Al2p for muscovite was larger than the instrumental error of 0.2 eV, which shown that the active sites on the muscovite surface for SP adsorption was Al atoms (Wang et al., 2021). For arsenopyrite, the chemical shifts of Fe2p3/2 (0.09 eV), Fe2p1/2 (0.08 eV), As3d5/2 (0.08 eV), As3d3/2 (0.12 eV) and O1s (0.07 eV) were all smaller than 0.2 eV, illustrating that the interaction between SP and arsenopyrite was very weak (Fantauzzi et al., 2011; Parthasarathy et al., 2014).

The adsorption of reagent on mineral surface would bring about new elements and cover up some surface atoms, resulting in the change of atomic content on mineral surface (Chen et al., 2020). Table 2 shows that before and after SP addition, the change of P and Al on the surface of muscovite was +1.72 and -1.62 respectively. It could be inferred that SP adsorbed through the P-O group with the Al sites on the surface of muscovite. While, before and after SP addition, the change of P on arsenopyrite surface was only +0.27, and the change of Fe and As was also slight. This phenomenon shown that SP adsorption on muscovite was stronger, which was consistent with the previous experimental results.

Table 1. Binding energy valence electrons on muscovite and arsenopyrite surfaces

Minerals	Element	Binding Energy/eV		Chemical Shift
		Without SP	Treated with SP	ΔE/eV
Muscovite	Al_{2p}	73.74	74.15	0.41
	Si_{2p}	101.83	101.84	0.01
	O_{1s}	531.12	531.12	0.00
Arsenopyrite	$Fe_{2p3/2}$	706.79	706.88	0.09
	$Fe_{2p1/2}$	711.21	711.29	0.08
	$As_{3d5/2}$	41.00	41.08	0.08
	$As_{3d3/2}$	44.37	44.49	0.12
	O_{1s}	530.62	530.55	0.07

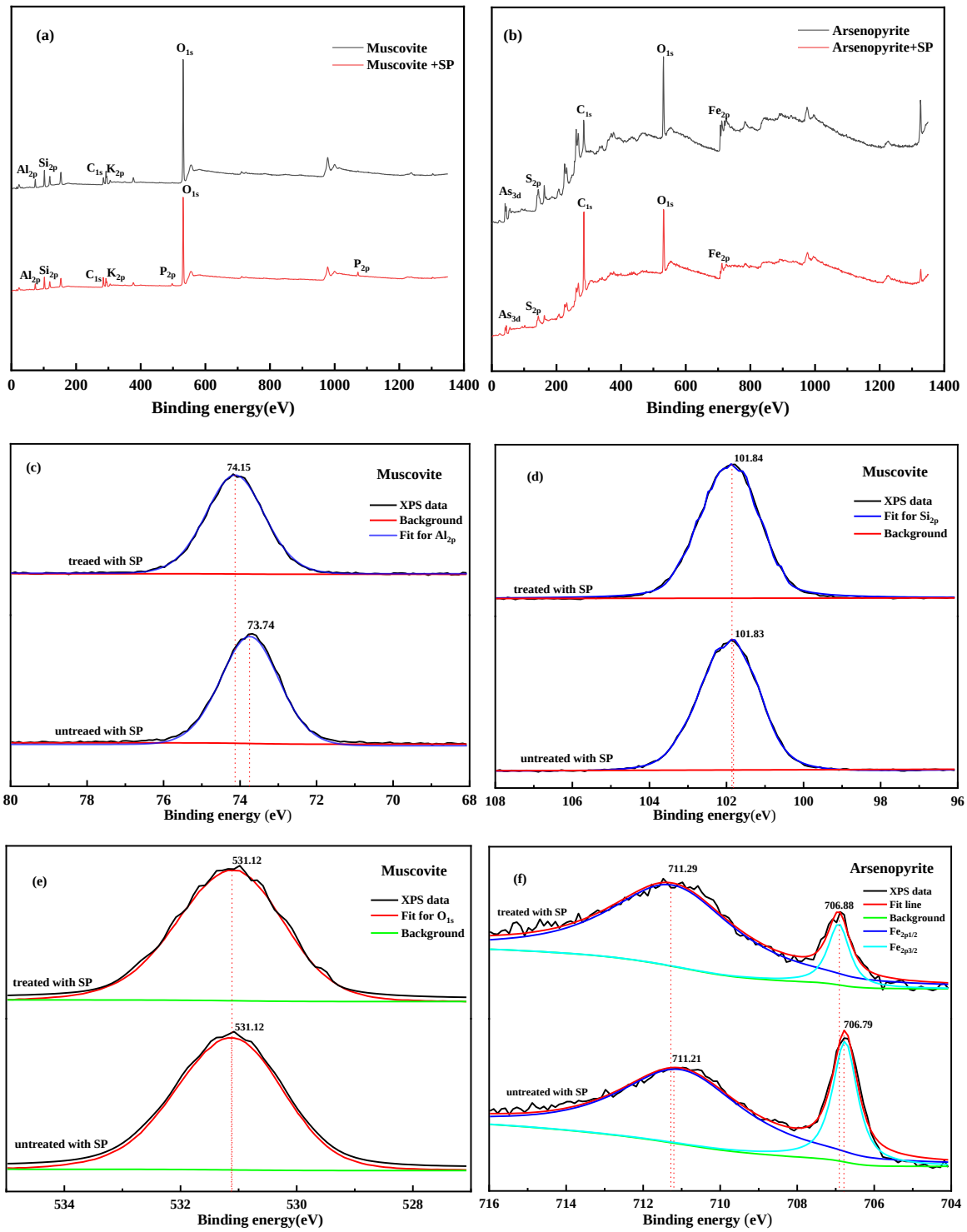

Fig. 12. (a) XPS spectra of muscovite surface; (b) XPS spectra of arsenopyrite surface; (c–e) XPS spectra of Al, Si, O, and on muscovite surface, respectively; (f–h) XPS spectra of Fe, As and O on arsenopyrite surface, respectively

Table 2. Relative contents of the elements on the minerals surface

Sample	Surface atomic composition (%)						
	P_{2p}	Al_{2p}	O_{1s}	C_{1s}	Si_{2p}	Fe_{2p}	As_{3d}
Muscovite	0	11.13	50.28	25.11	13.48	–	–
Muscovite+SP	1.72	9.51	50.93	24.4	13.44	–	–
Arsenopyrite	–	–	35.6	39.33	–	11.74	13.33
Arsenopyrite +SP	0.27	–	35.43	39.18	–	11.85	13.27

3.6. Suggested adsorption model

A possible interfacial interaction model of SP and IAX in arsenopyrite/muscovite system is given in Fig. 13. With xanthate as the collector, the flotability of arsenopyrite was well but that of muscovite was poor because the selective adsorption of IAX, so it seems that they can be separated by flotation without additional reagents. However, for mixed mineral flotation fine muscovite will adsorb on arsenopyrite surface through heterocoagulation, reducing the adsorption of IAX on arsenopyrite surface by covering the active sites for IAX adsorption, hence decreasing its flotability. When SP was added before the addition of IAX, SP was adsorbed on muscovite surface by the interaction between its P-O groups with the Al sites on muscovite surface, so as to disperse muscovite by the strengthened electrostatic repulsion and make it couldn't cover on arsenopyrite. The adverse effect of muscovite on arsenopyrite was eliminated by SP and the adsorption of IAX on arsenopyrite was recovered, so it was re-floated.

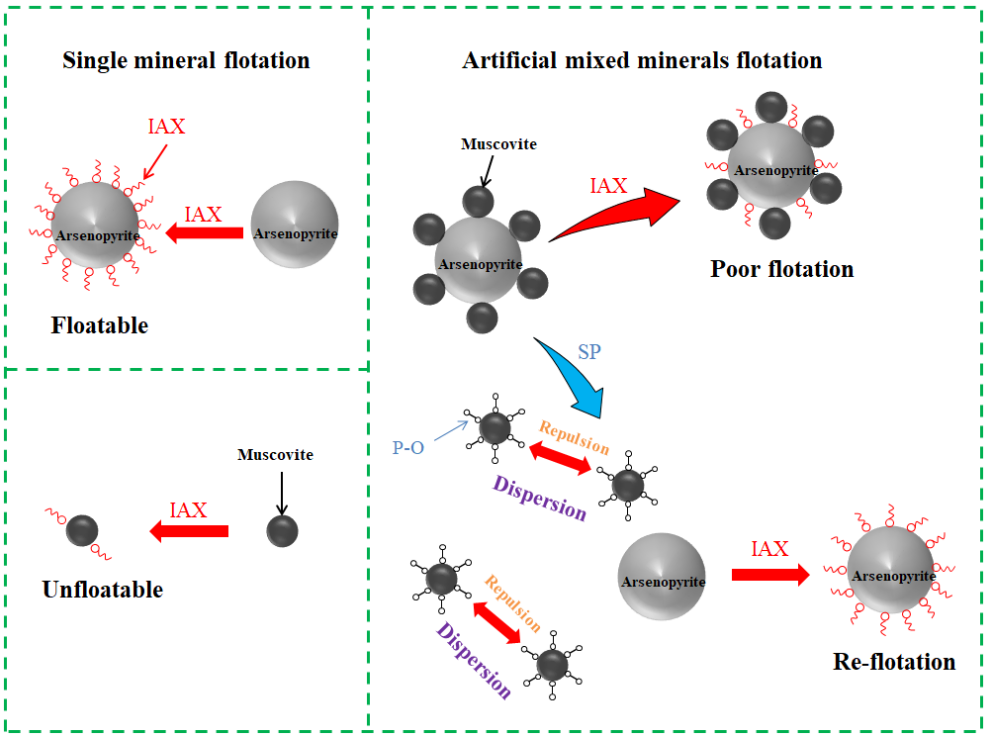

Fig. 13. Possible interaction mechanisms of SP improved the flotation of arsenopyrite/muscovite system

4. Conclusion

The flotation of arsenopyrite was poor in the mixed arsenopyrite/muscovite system although it floated well in single system. This was ascribed to the adverse effect of the coverage of muscovite on arsenopyrite surface. By adding SP in the mixed system the flotation of arsenopyrite recovered to a great extent, i.e. SP eliminated this coverage effect.

For the mixed system, the adsorption of IAX on arsenopyrite decreased, due to the occupancy of fine muscovite particles on the active sites of arsenopyrite surface, which resulting in the declined flotability. When SP was introduced it selectively adsorbed on muscovite surface by the interaction between its P-O groups and the Al active sites of muscovite. This reduced the zeta potential of muscovite and increased the repulsion between muscovite particles, and realized its dispersion. So the adsorption of IAX on arsenopyrite and the flotability recovered. SP was qualified as a dispersant for flotation separation of arsenopyrite and muscovite.

Acknowledgements

The authors acknowledge the support of the Sichuan Science and Technology Program of China (No. 2021YFG0269, 2022YFQ0074, 2022YFS0453), and the Doctoral Foundation of Southwest University of Science and Technology, China (No. 20ZX7149).

References

CHANTURIYA, V.A., BUNIN, I.Z., RYAZANTSEVA, M.V., FILIPPOV, L.O., 2011. *Theory and applications of high-power nanosecond pulses to processing of mineral complexes*, Mineral Processing Extractive Metallurgy Review, 32, 105-136.

CHANTURIA, V.A., IVANOVA, T.A., GETMAN, V.V., KOPORULINA, E.V., 2015. *Methods of minerals modification by the micro-and nanoparticles of gold and platinum for the evaluation of the collectors selectivity at the flotation processing of noble metals from the fine ingrained ores,* Mineral Processing and Extractive Metallurgy Review, 36, 288-304.

CHEN, Y., SHI, Q., FENG, Q., LU, Y., ZHANG, W., 2017. *The Effect of Conditioning on the Flotation of Pyrrhotite in the Presence of Chlorite*, Minerals, 7, 125.

CHEN, W., FENG, Q., ZHANG, G., YANG, Q., 2018. *Investigations on flotation separation of scheelite from calcite by using a novel depressant: Sodium phytate*, Minerals Engineering, 126,116-122.

CHEN, X., PENG, Y., 2018. *Managing clay minerals in froth flotation – A critical review*, Mineral Processing and Extractive Metallurgy Review, 39, 289-307.

CHEN, H., LI, Q., WANG, M., JI, D., TAN, W., 2020. *XPS and two-dimensional FTIR correlation analysis on the binding characteristics of humic acid onto kaolinite surface*, Science of the Total Environment, 724, 138154.

DENG, S., GU, G., XU, B., LI, L., WU, B., 2018. *Surface characterization of arsenopyrite during chemical and biological oxidation*, Science of the Total Environment, 626,349-356.

DENG, S., YAN, C., GUO, K., GU, G., 2022. *Influence of Ferric Ions on the Electrochemical Dissolution Behaviors of Arsenopyrite in Sulfuric Acid of pH 1*, Mineral Processing and Extractive Metallurgy Review, 43, 728-732.

FANTAUZZI, M., LICHERI, C., ATZEI, D., LOI, G., ELSENER, B., ROSSI, G., ROSSI, A., 2011. *Arsenopyrite and pyrite bioleaching: evidence from XPS, XRD and ICP techniques,* Analytical and Bioanalytical Chemistry, 401, 2237-2248.

FENG, B., FENG, Q., LU, Y., 2012. *A novel method to limit the detrimental effect of serpentine on the flotation of pentlandite,* International Journal of Mineral Processing, 114, 11-13.

FERLIN, N., GRASSI, D., OJEDA, C., CASTRO, M.J., CIRELLI, A.F., KOVENSKY, J., GRAND, E., 2015. *Octyl glucoside derivatives: A tool against metal pollutants,* Colloids and Surfaces A: Physicochemical and Engineering Aspects, 480, 439-448.

FENG, B., PENG, J., ZHANG, W., LUO, G., WANG, H., 2018. *Removal behavior of slime from pentlandite surfaces and its effect on flotation,* Minerals Engineering, 125, 150-154.

HUANG, J., XIONG, S., LONG, Q., SHEN, L., WANG, Y., 2018. *Evaluation of food additive sodium phytate as a novel draw solute for forward osmosis*, Desalination, 448, 87-92.

HUANG, Q., LI, X., REN, S., LUO, W., 2019. *Removal of ethyl, isobutyl, and isoamyl xanthates using cationic gemini surfactant-modified montmorillonites*, Colloids and Surfaces A-Physicochemical and Engineering Aspects, 580, 123723.

LU, J., TONG, Z., YUAN, Z., LI, L., 2019. *Investigation on flotation separation of chalcopyrite from arsenopyrite with a novel collector: N-Butoxycarbonyl-O-Isobutyl Thiocarbamate*, Minerals Engineering, 137, 118-123.

LOPÉZ, R., JORDÃO, H., HARTMANN, R., ÄMMÄLÄ, A., CARVALHO, M.T. 2019. *Study of butyl-amine nanocrystal cellulose in the flotation of complex sulphide ores*, Colloids and Surfaces A: Physicochemical and Engineering Aspects, 579, 123655.

MING, P., XIE, Z., GUAN, Y., WANG, Z., LI, F., XING, Q., 2020. *The effect of polysaccharide depressant xanthan gum on the flotation of arsenopyrite from chlorite*, Minerals Engineering, 157, 106551.

PARTHASARATHY, H., BALTRUS, J. P., DZOMBAK, D. A., KARAMALIDIS, A. K., 2014. *A method for preparation and cleaning of uniformly sized arsenopyrite particles,* Geochemical Transactions, 15, 1-7.

RAMIREZ, A., ROJAS, A., GUTIERREZ, L., LASKOWSKI, J.S., 2018. *Sodium hexametaphosphate and sodium silicate as dispersants to reduce the negative effect of kaolinite on the flotation of chalcopyrite in seawater*, Minerals Engineering, 125, 10-14.

THAKUR D.N., SAROJ K.K., GUPTA A., 1995 *Biological pretreatment of arsenopyrite tailings and its effect on cyanide leaching of gold,* Mineral Processing and Extractive Metallurgy Review, 15. 87-93.

TANG, X., CHEN, Y., 2020. *Using oxalic acid to eliminate the slime coatings of serpentine in pyrite flotation*, Minerals Engineering, 149, 106228.

WANG, B., PENG, Y., VINK, S., 2013. *Diagnosis of the surface chemistry effects on fine coal flotation using saline water,* Energy & Fuels, 27, 4869-4874.

WANG, L., SUN, W., HU, Y. H., XU, L.H., 2014. *Adsorption mechanism of mixed anionic/cationic collectors in Muscovite–Quartz flotation system,* Minerals Engineering, 64, 44-50.

WANG, X., ZHAO, K., BO, H., YAN, W., WANG, Z., GU, G., GAO, Z., 2020. *Improved flotation of auriferous arsenopyrite by using a novel mixed collector in weakly alkaline pulp*, Physicochemical Problems of Mineral Processing, 56.

WANG, D., LIU, Q., 2021. *Influence of aggregation/dispersion state of hydrophilic particles on their entrainment in fine mineral particle flotation*, Minerals Engineering, 166, 106835.

WANG, Y., WANG, Y., WEN, K., DANG, W., XUN, J., 2021. *Strengthening the inhibition effect of sodium silicate on muscovite by electrochemical modification*, Minerals Engineering, 161, 106731.

WANG, Z., CAO, J., WANG, L., XIAO, J., WANG, J., 2021. *Selective depression of arsenopyrite with in situ generated nanoparticles in pyrite flotation*, Minerals Engineering, 173, 107223.

YAO, J., YIN, W., GONG, E., 2016. *Depressing effect of fine hydrophilic particles on magnesite reverse flotation,* International Journal of Mineral Processing, 149, 84-93.

YU, L., LIU, Q., LI, S., DENG, J., LUO, B., LAI, H., 2019. *Depression mechanism involving Fe3+ during arsenopyrite flotation*, Separation and Purification Technology, 222, 109-116.

ZHAO, K., YAN, W., WANG, X., WANG, Z., GAO, Z., WANG, C., HE, W., 2020. *Effect of a novel phosphate on the flotation of serpentine-containing copper-nickel sulfide ore,* Minerals Engineering, 150, 106276.

ZHANG, X., HAN, Y., GAO, P., GU, X., WANG, S., 2020. *Depression Mechanism of a Novel Depressant on Serpentine Surfaces and Its Application to the Selective Separation of Chalcopyrite from Serpentine*, Mineral Processing and Extractive Metallurgy Review, 1-7.

ZHANG, Y., LI, Q., SUN, S., LIU, X., JIANG, T., LYU, X., HE, Y. 2021. *Electrochemical behaviour of the oxidative dissolution of arsenopyrite catalysed by Ag+ in 9K culture medium*, Colloids and Surfaces A: Physicochemical and Engineering Aspects, 614, 126169.

ZHANG, Q., WEN, S., FENG, Q., LIU, Y., 2021. *Activation mechanism of lead ions in the flotation of sulfidized azurite with xanthate as collector*, Minerals Engineering, 163, 106809.

ZHANG, Y., ZHANG, B., CHEN, Y., YUAN, B., ZHANG, W., SHANG, S., 2021. *Effectiveness and mechanism of sodium phytate as a green inhibitor for the dust deflagration of lysine sulfate*, Process Safety and Environmental Protection, 147, 772-787.